International Journal of Hydrogen Energy 180 (2025) 151694

Contents lists available at ScienceDirect

International Journal of Hydrogen Energy

journal homepage: www.elsevier.com/locate/he

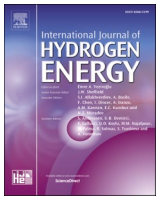

Catalytic hydrogen combustion as heat source for the dehydrogenation of liquid organic hydrogen carriers using a novel compact autothermal reactor

C. Gescher [a], S. Hahn [a,b], C. Hornung [c], M. Weiss [a,b], T. Rüde [a], M. Geißelbrecht [a], P. Wasserscheid [a,b,d,*]

[a] Forschungszentrum Jülich, Helmholtz-Institute Erlangen-Nürnberg for Renewable Energy (IET 2), Cauerstraße 1, 91058, Erlangen, Germany
[b] Forschungszentrum Jülich, Institute for a Sustainable Hydrogen Economy, Marie-Curie-Straße 5, 52428, Jülich, Germany
[c] CSIRO Manufacturing, Private Bag 10, Clayton South, Victoria, 3169, Australia
[d] Lehrstuhl für Chemische Reaktionstechnik, Friedrich-Alexander-Universität Erlangen-Nürnberg, Egerlandstr. 3, 91058, Erlangen, Germany

ARTICLE INFO

Handling Editor: A Bhatnagar

Keywords:
Hydrogen storage
Perhydro benzyltoluene
Catalytic hydrogen combustion
Autothermal reactor design

ABSTRACT

The experimental performance of an autothermal hydrogen release unit comprising a perhydro benzyltoluene (H12-BT) dehydrogenation chamber and a catalytic hydrogen combustion (CHC) chamber in thermal contact is discussed. In detail, the applied set-up comprised a multi-tubular CHC heating based on seven parallel tubes with the reactor shell containing a commercial dehydrogenation catalyst. In this way, the CHC heated the endothermal LOHC dehydrogenation using a part of the hydrogen generated in the dehydrogenation. The proposed heating concept for autothermal LOHC dehydrogenation offers several advantages over state-of-the-art heating concepts, including minimized space consumption, high efficiency, and zero NO_x emissions. During performance tests the process reached a minimum hydrogen combustion fraction of 37 %, while the minimum heat requirement for the dehydrogenation reaction for industrial scale plants is 33 %. The reactor orientation (vertical vs horizontal) and the flow configuration (counter-current vs. co-current) showed very little influence on the performance demonstrating the robustness of the proposed reactor design.

1. Introduction

The transition of our energy system to a fully defossilized one is vital for dealing with the enormous challenge of climate change [1]. Besides a further expansion of renewable power generation this requires significant developments in energy storage and energy transport capabilities to align fluctuating power generation with energy demand. For day-night storage cycles and the GWh range, electrochemical, mechanical, and thermal storage systems can provide solutions [2]. However, for even larger scales and longer storage durations chemical storage systems, such as hydrogen, methane or liquid hydrocarbons, are more adequate due to their much higher gravimetric energy densities [3,4]. Liquid chemical energy storage systems can even be used as drop-in replacements that allow the further utilization of the existing fuel infrastructure saving large amounts of investment in new infrastructures.

Hydrogen is a very interesting fuel for the defossilized energy system of the future due to its high gravimetric energy content and non-toxic nature [5]. The low volumetric energy content of molecular hydrogen at ambient conditions is, however, a challenge for many practical use cases [6]. Traditional ways to increase the volumetric energy density by compression or liquefaction come with energy requirements and the need for new infrastructures, such as pressure vessels, pipelines or cryogenic containers [7].

Liquid organic hydrogen carrier (LOHC) systems allow the storage and transport of hydrogen in a chemically bound state in the form of liquids. Additionally, LOHC technologies enable safe and easy hydrogen handling, while attaining similar volumetric energy densities to physical hydrogen storage technologies [7–9]. They are considered as a viable and competitive solution for large-scale hydrogen storage and transport [10–13]. One characteristic feature of LOHC technologies is the endothermal character of the hydrogen release reaction. In the case of perhydro benzyltoluene (H12-BT) dehydrogenation, the hydrogen release consumes at least 26 % of the lower heating value (LHV) of the released hydrogen. The same amount of heat is released in the reverse hydrogenation of benzyltoluene (H0-BT) which is the corresponding hydrogen storage reaction of the LOHC system [14]. For thermodynamic reasons,

* Corresponding author. Forschungszentrum Jülich, Helmholtz-Institute Erlangen-Nürnberg for Renewable Energy (IET 2), Cauerstraße 1, 91058, Erlangen, Germany.
E-mail address: p.wasserscheid@fz-juelich.de (P. Wasserscheid).

https://doi.org/10.1016/j.ijhydene.2025.151694
Received 9 July 2025; Received in revised form 4 September 2025; Accepted 22 September 2025
Available online 30 September 2025

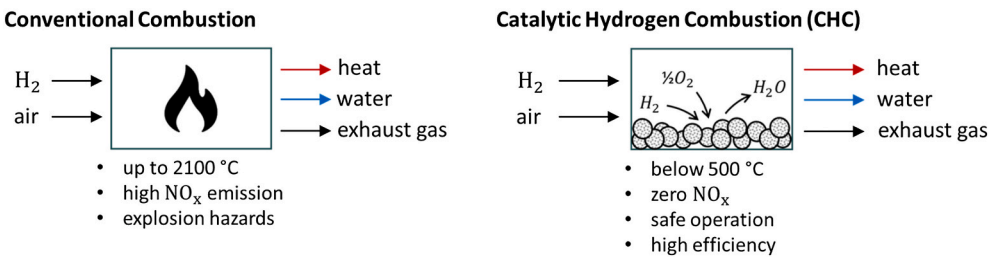

Fig. 1. Schematic depiction of conventional hydrogen combustion and catalytic hydrogen combustion, highlighting the advantages of CHC as a heat supply concept for LOHC dehydrogenation.

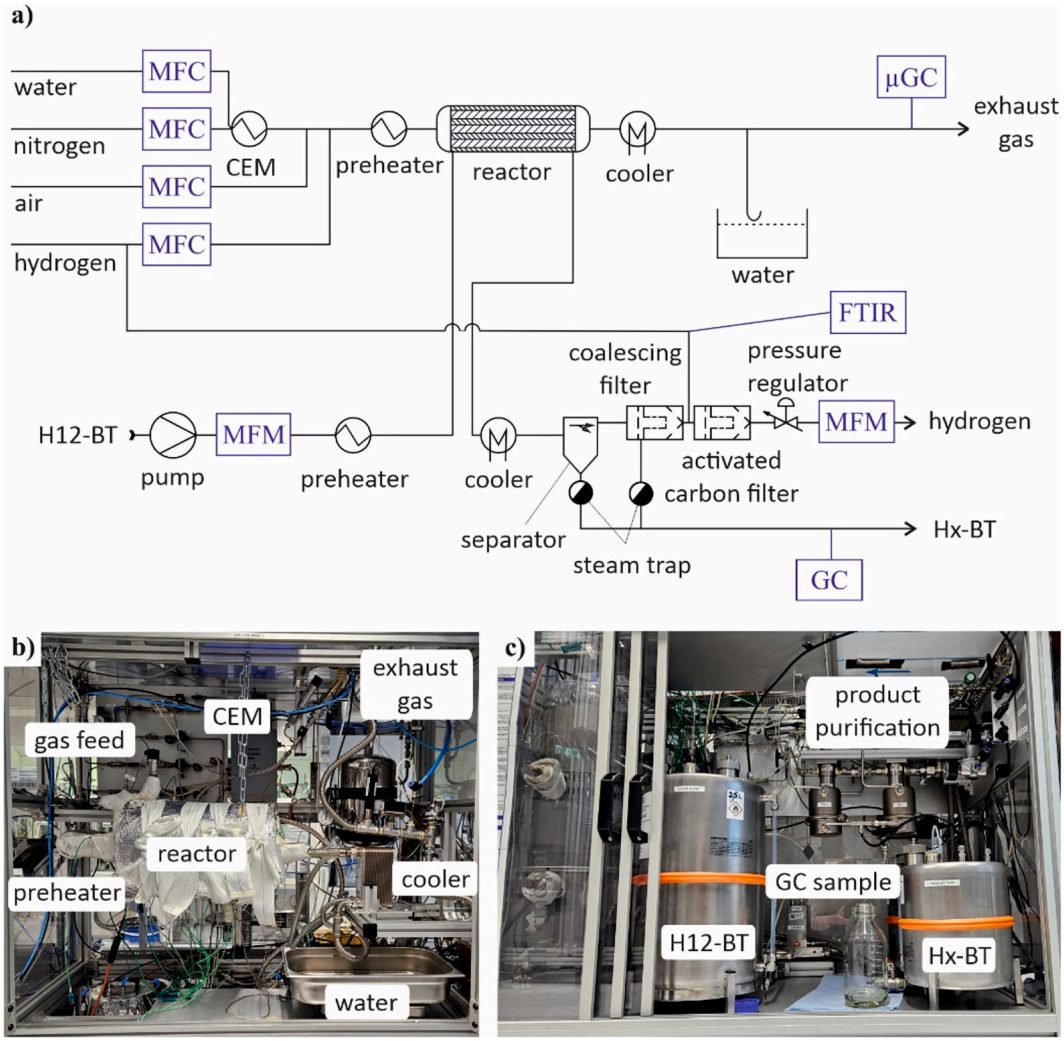

Fig. 2. a) Simplified flow diagram of the applied dehydrogenation plant with CHC. Nitrogen and water are fed into the hydrogen-containing gas mixture to mimic exhaust gas recirculation. CEM: controlled evaporator mixer, µGC: micro gas chromatograph, MFC: mass flow controller, FTIR: Fourier transform infrared spectroscope, PID: photoionization detector. b) Upper part of the plant with the combustion periphery and insulated reactor. The preheating zone is located behind the reactor and is covered by it. **c)** Lower part of the plant with the dehydrogenation periphery. The product purification consists of coalescing filter, activated carbon filter separator and steam trap. The preheater is installed in the insulation in the immediate vicinity of the reactor.

the heat for hydrogen release must be provided at a relatively high temperature level (>280 °C for H0-BT/H12-BT), which makes the usage of waste heat in many application cases difficult [15,16].

Efficient and compact heat supply is therefore a major challenge for a technically feasible implementation of the LOHC technology, especially if the hydrogen is to be provided on mobile platforms, such as coastal ships, river barges, trains or heavy-duty vehicles [9,17]. In this context, autothermal reactor concepts that thermally combine the endothermal dehydrogenation reaction with an exothermal reaction in adjacent process chambers have been shown to significantly increase the power density of hydrogen provision from LOHC systems [12,18].

Another point for optimization is the space-time-yield of the combined dehydrogenation/heat provision process unit. Kadar et al. have proposed an inverted fixed-bed reactor design for H12-BT dehydrogenation [19] that increases the catalyst volume – and with that the produced amount of hydrogen - in the same reactor volume by a factor of

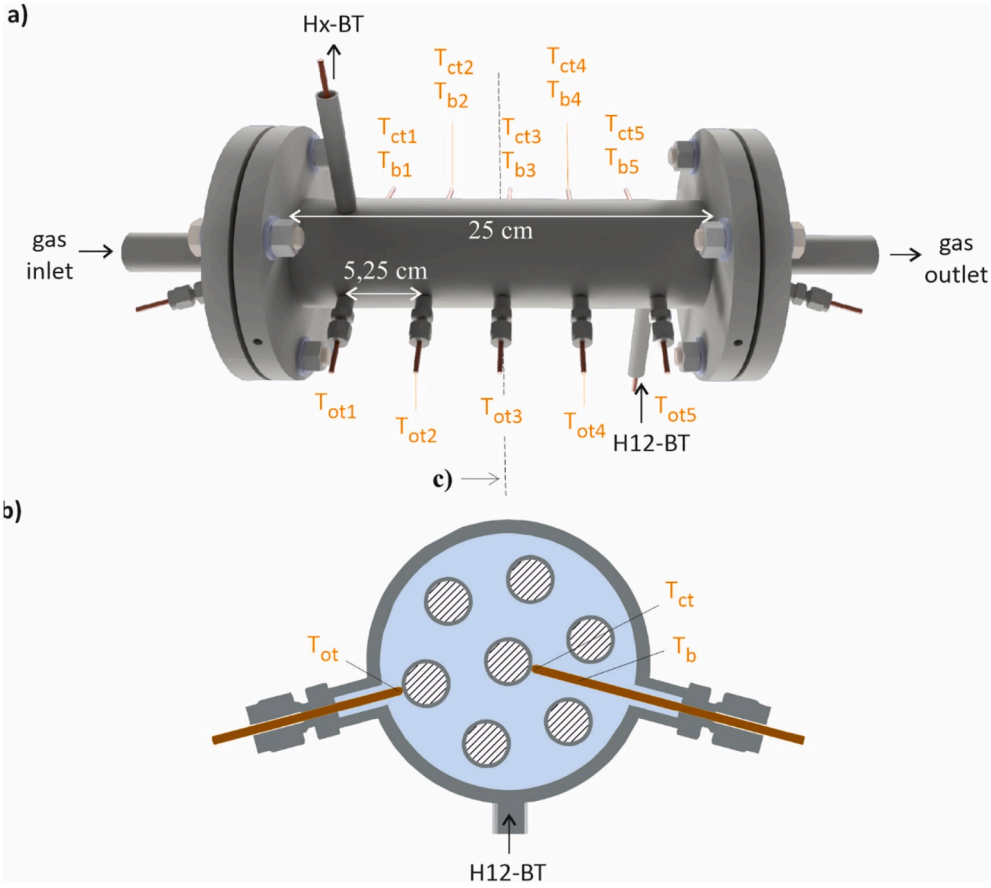

Fig. 3. a) 3D image of the tube bundle reactor with 7 tubes. The combustion in the tubes heats the dehydrogenation in the shell. Thermocouples contacting an outer tube (T_{ot1}-T_{ot5}) are shown at the front. At the rear are double thermocouples that contact the central tube (T_{ct1}-T_{ct5}) and have an extra measuring point in the catalyst bed (T_{b1}–T_{b5}). The gas temperature is measured at the gas inlet and gas outlet. **b)** Cross-section of the tube bundle through the third temperature measuring point to illustrate the thermocouple position within the bundle.

two. Wang et al. introduced catalytic hydrogen combustion (CHC) as a heat source for LOHC dehydrogenation reactors and replaced in this way the space-consuming external heating of a heat transfer fluid [20]. Their experiments with the methylcyclohexane-based LOHC system were conducted in a simple double jacket tubular reactor and showed that a self-sustained hydrogen release process is possible.

CHC offers several advantages compared to conventional free-flame hydrogen combustion when used as heat source in LOHC dehydrogenation reactions as summarized in Fig. 1. Due to the catalytic nature of hydrogen oxidation, the resulting combustion temperatures are much lower than in conventional free-flame combustion. Hereby, typical CHC temperature levels (300–500 °C) offer an excellent fit to the required temperature level for LOHC dehydrogenation [21]. This perfect match allows for direct heat coupling with the dehydrogenation reaction which increases the power density of the system compared to the conventional free-flame heating with a thermal oil cycle. The lower combustion temperatures also result in a cleaner hydrogen combustion process with zero NO_x emissions [22–25]. CHC systems use precious metal catalysts, such as platinum or palladium, in tiny little amounts as active catalyst components [21–23]. A challenge with CHC is to combine high thermal efficiency with safe operation without flame formation. As recently shown, this challenge can be overcome by using an external exhaust gas recirculation concept that enables stoichiometric combustion while operating below the explosive concentration range [26].

Thus, a combination of CHC and the inverted multi-tubular reactor design promises an impressive optimization potential in terms of volumetric power density for autothermal dehydrogenation of LOHC material. This work will present a highly innovative conceptual proposal for an autothermal reactor combining the two technologies and will deliver the first proof-of-concept of the coupled process in a continuous lab-scale demonstration plant.

2. Methods & experiments

The applied lab-scale dehydrogenation unit combines a CHC compartment with a dehydrogenation compartment in a single reactor shell. While gas mixtures containing hydrogen, air, nitrogen and/or steam are fed to the CHC compartment, H12-BT in various qualities are pumped into the dehydrogenation compartment. The plant enables variation of process parameters, such as H_2 fraction in the combustion gas, H12-BT flow rate, preheating temperature or reactor pressure. Moreover, the unit allows us to change orientation of the reactor (vertical/horizontal) and of flow directions in the combustion and dehydrogenation zone (cocurrent/countercurrent). Fig. 2 shows the simplified flow diagram of the coupled process and a photo of the experimental plant setup as used for this work. Hx-BT refers to the technical mixture of dehydrogenated BT with a remaining amount of hydrogen.

Our aim is to study the influence of the above-named process parameters on process performance and the demonstration of an efficient and reliable autothermal hydrogen provision process.

In the combustion section, the molar flow rates of nitrogen (N_2), synthetic air, and hydrogen (H_2) (each with 5.0 purity, synthetic air consisting of 80 % N_2 and 20 % O_2) are adjusted using mass flow controllers (MFCs). For the vapor fraction, that is used to simulate off-gas recirculation, deionized water is fed from a pressurized 11-L water

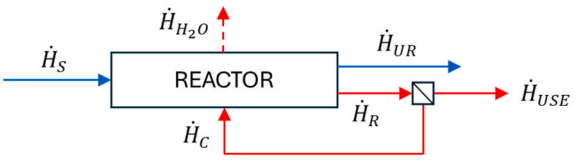

Fig. 4. Hydrogen flow diagram through the autothermal reactor system applied in this work.

tank into a controlled evaporator mixer (CEM). The water flow is controlled using an MFC, which consists of a Coriolis mass flow meter (MFM) in combination with a control valve at the CEM. In the CEM, the liquid water is dispersed into the nitrogen stream and then heated and evaporated. Air and hydrogen are added in the preheating section and all gases are mixed in a static mixer. The preheating temperature is set to the outer tube temperature, which is limited to 400 °C. In summary, the electrical preheating and the addition of extra nitrogen and water vapor are laboratory surrogates that mimic heat recuperation and exhaust-gas recirculation foreseen at scale. After heating, the gas mixture enters the CHC compartment of the reactor. This consists of seven individual tubes (250 mm length, 10 mm inner diameter, 12 mm outer diameter) containing the CHC catalyst. The CHC tubes are aligned in a circle of six outer tubes and one inner tube, as depicted in Fig. 3. The tubes are filled with a total of 56.9 g Neoxid platinum mesh catalyst (Pt loading 0.14 wt.-%). A spiraled mesh was inserted coaxially into each tube. This catalyst was chosen for its simple sizing, which is achieved through easy cutting and rolling. The spring tension of the spiral also makes insertion and removal easy, while its design reduces pressure drop and hot spot formation. The amount of catalyst was chosen to guarantee complete hydrogen conversion. Ten thermocouples are installed in the CHC compartment to measure the temperatures at different positions during operation. As shown in Fig. 3, the temperature of the center tube and the temperature of one of the outer tubes is tracked along the reactor axis at five points. The hot flue gas leaving the CHC compartment is cooled in a water-cooled heat exchanger to a temperature below 20 °C. During cooling, the majority of the water vapor in the flue gas condenses and is removed from the system via a siphon. Up- and downstream of the CHC compartment, several measurement devices ensure a continuous monitoring of essential process parameters, such as the combustion gas inlet and outlet temperatures as well as the pressure drop along the reactor. Gas phase samples of the combustions process are taken from the exhaust gas and are processed continuously during the entire process by an online μGC. An exemplary chromatogram is shown in Fig. S6 in the SI.

The dehydrogenation section of the rig includes tanks for H12-BT and Hx-BT. From the H12-BT tank, H12-BT is pumped to the reactor using a micro-gear pump controlled by a Coriolis MFM. Subsequently, H12-BT is preheated electrically in a coiled capillary before entering the dehydrogenation compartment of the reactor located in the reactor shell surrounding the CHC tubes. The electric preheater mimics the heat recuperation foreseen at scale. The dehydrogenation compartment contains 350 g of the dehydrogenation catalyst EleMax D102 from Clariant Produkte GmbH, Germany. Five thermocouples measure the reactor temperature in the catalyst bed at different positions along the axial length of the reactor (see Fig. 3). The hot reaction mixture leaving the dehydrogenation compartment consists of a mixture of liquid and vaporized Hx-BT and hydrogen. This gaseous mixture is led to a heat exchanger cooled with cold water (15 °C) where the Hx-BT vapor condenses. In the subsequent separator and coalescence filter, Hx-BT droplets are separated from gaseous hydrogen. A certain share of the produced hydrogen is separated after the coalescence filter and redirected into the combustion compartment of the reactor. The hydrogen fraction used for combustion is variable. Gas phase samples of the released hydrogen are taken between the coalescing filter and the combustion process and are measured by a Fourier transform infrared spectroscope (FTIR).

The condensed Hx-BT is directed from the separator to the product tank via a condensate drain. At this point, a sample is taken for gas chromatographic analysis of the Hx-BT to determine its degree of dehydrogenation and its methyl fluorene content. The portion of hydrogen that is not burned is further cleaned from volatile organic compounds (VOCs) in an activated carbon filter to protect the subsequent MFM. The MFM quantifies the hydrogen flow and provides online information about the actual hydrogen production.

The operating pressure of the dehydrogenation is set by a pressure controller located behind the activated carbon filter. In this way, the entire downstream section of the unit is operated under the hydrogen pressure of the dehydrogenation compartment.

2.1. Experimental procedure

The shell side dehydrogenation compartment of the reactor is flushed with hydrogen before starting the experiment to ensure a reproducible starting point of the operation. Then, hydrogen is fed first from the gas bottle into the CHC compartment and the combustion heat starts to heat up the reactor. Once the temperature at the hottest measurement point in the reactor reaches 320 °C, the H12-BT feeding is initiated and hydrogen is released from the dehydrogenation compartment. As soon as the released hydrogen flow corresponds to the hydrogen feed flow for the combustion the hydrogen supply for the combustion is switched from the gas bottle to the hydrogen released from the dehydrogenation compartment.

In our set-up, the time for initial start-up from cold to steady-state H12-BT dehydrogenation took approximately 120 min. For subsequent changes in process parameters, we waited 40–90 min to ensure that the new steady-state was reached and that the Hx-BT sample taken was representative for this new steady-state. For each set of process parameters, two Hx-BT samples were taken.

2.2. Reference configuration

The reference configuration for the dehydrogenation side was defined by a H12-BT flow rate of 10 g min^{-1} and a pressure of 2 barg in the reactor. The reference temperature of the preheated gas flow at the reactor inlet was set to 350 °C at the tube temperature. Gas inlet temperature was slightly below. The reference combustion gas mixture corresponded to a combustion heat of 375 W with a total flow of 70 sL min^{-1}, containing 3 mol% H_2, 2 mol% O_2, 64 mol% N_2 and 31 mol% H_2O. Thus, the combustion gas mixture was close to stoichiometric. Concerning the reactor setup in the coupled process, the reference configuration was horizontal countercurrent, i.e., the reactor was aligned horizontally and the combustion gas and LOHC were flowing in opposite directions, as illustrated in Fig. 3a.

2.3. Key performance indicators (KPIs)

Several KPIs are used to evaluate the process performance under varying process conditions and to compare the autothermal process to other heating concepts for H12-BT dehydrogenation. The majority of these KPIs are derived from the hydrogen molar flowrates in the reactor on both the dehydrogenation and the combustion side. In the interest of simplicity, these hydrogen flowrates will be described with $\dot{H}$ from here onwards. These molar flowrates should not be confused with enthalpy terms; they have the unit sL min^{-1}. Fig. 4 depicts a flow diagram showing these hydrogen flows through the autothermal reactor system.

From Fig. 4 the following hydrogen balances can be derived for the dehydrogenation compartment:

$$\dot{H}_S = \dot{H}_R + \dot{H}_{UR} = \dot{H}_{USE} + \dot{H}_C + \dot{H}_{UR} \quad (1)$$

For the combustion compartment the hydrogen balance reads:

$$\dot{H}_C = \dot{H}_{H_2O} \quad (2)$$

with the hydrogen flows being.

$\dot{H}_S$ - flow of reversibly stored hydrogen in the H12-BT feed
$\dot{H}_R$ - flow of released gaseous hydrogen exiting the dehydrogenation compartment
$\dot{H}_{UR}$ - flow of non-released hydrogen exiting the dehydrogenation compartment, still stored within the Hx-BT product stream
$\dot{H}_{USE}$ - flow of useable hydrogen gas resulting from the subtraction of the hydrogen used for combustion from the total amount of hydrogen released
$\dot{H}_C$ - flow of hydrogen gas fed back into the combustion compartment of the reactor
$\dot{H}_{H_2O}$ - flow of hydrogen oxidized to water in the combustion compartment of the reactor.

2.3.1. Degree of dehydrogenation (DoD)

The Degree of Dehydrogenation (DoD) is defined as the ratio of released hydrogen to the total amount of reversibly stored in a given Hx-BT mixture. In the hydrogen release reaction, a high DoD in the product mixture is desirable as this corresponds to a high utilization of the LOHC storage capacity. To determine the DoD, the released hydrogen flow is measured and compared to the amount of reversible stored hydrogen in the H12-BT feedstock (equation (4)).

$$DoD = \frac{\dot{H}_R}{\dot{H}_S} \quad (3)$$

Apart from the determination via the product hydrogen flow measurement, the DoD can also be determined via liquid analysis of the Hx-BT product via gas chromatography.

2.3.2. Hydrogen combustion fraction (HCF)

The hydrogen combustion fraction (HCF) describes the ratio of hydrogen utilized for heat production in the CHC compartment to the total amount of released hydrogen:

$$HCF = \frac{\dot{H}_C}{\dot{H}_R} \quad (4)$$

A lower hydrogen combustion fraction represents a lower loss in hydrogen/energy. 1-HCF can be used as energy or hydrogen efficiency. A low HCF means high efficiency and is therefore desirable.

2.3.3. Storage efficiency (SE)

A crucial KPI to evaluate the autothermal hydrogen release is the storage efficiency (SE). It is calculated as the ratio of useable hydrogen flow to the amount of hydrogen stored in the LOHC material:

$$SE = \frac{\dot{H}_{USE}}{\dot{H}_S} = \frac{\dot{H}_R - \dot{H}_C}{\dot{H}_S} = (1 - HCF)*DoD \quad (5)$$

The storage efficiency combines the assessment of the dehydrogenation process and the combustion process. It can be calculated from the HCF and the DoD, as shown in equation (5).

2.3.4. Relative heating power (RHP)

The relative heating power *(RHP)* describes the share of hydrogen utilized in the CHC compartment to heat the reactor for hydrogen release:

$$RHP = \frac{\dot{H}_C}{\dot{H}_S} \quad (6)$$

2.3.5. Product quality of the liquid phase

To evaluate the cyclic stability of the LOHC system in use, it is essential to analyze the side products in the liquid product phase. Therefore, all liquid samples are analyzed for the most relevant side product methyl fluorene using gas chromatography (GC). The applied GC is a TRACE 1310 from Thermo Fisher Scientific equipped with a 30 m long Rxi-17Sil column.

2.3.6. Product quality of the gas phase

The analysis of side products in the product gas mixture from the dehydrogenation compartment is performed using FTIR spectroscopy. The gas phase is analyzed for volatile organic compounds (VOCs), such as toluene, benzene, methylcyclohexane and cyclohexane, as well as for CO and CO_2. For this purpose, the FTIR spectrometer type MultiGas™ 2031 from MKS Instruments is employed. The quantification is performed using the provided software and a library of existing calibration files for the named side products.

3. Results & discussion

3.1. Proof-of-concept and comparison with other dehydrogenation concepts

The proposed reactor concept for autothermal dehydrogenation brings several advantages compared to state-of-the-art heating concepts like electrical heating and conventional free-flame hydrogen combustion with a thermal oil cycle. The combination of CHC and the inverted reactor design promises a very high volumetric power density while enabling high efficiency as well as safe and emission-free operation.

3.1.1. Volumetric power density

Contrary to conventional free-flame combustion, where high temperature levels are reached, the CHC process enables heat provision at a temperature level that perfectly fits the requirements of the LOHC dehydrogenation. From this results the opportunity for direct heating saving the external heat transfer fluid cycle which was reported to account for around 30 % of the overall plant volume in the case of H12-BT dehydrogenation using a free-flame hydrogen combustion for heating [27]. According to our assumptions, by replacing the components needed for the external thermal oil cycle with the components needed for the here-proposed direct CHC heating the required volume can be reduced to one fifth [28]. Additionally, the inverted reactor design provides a higher catalyst volume per total reactor volume compared to conventional tubular reactor, increasing the power density in addition by up to 100 % [19]. Thus, the combination of the CHC heat provision with the inverted reactor design gives access to an autothermal hydrogen release concept with maximized volumetric power density.

3.1.2. Heating efficiency

For large industrial plants, a heat requirement of 11 kWh per kilogram of hydrogen released from H12-BT has been described as a realistic target [29,30]. This corresponds to a minimum hydrogen combustion fraction HCF of 33 %, assuming that the heat is fully transferred to the dehydrogenation reaction without losses. Willer et al., for example, investigated the heat consumption of the H12-BT dehydrogenation reaction in detail [16]. For conventional free-flame hydrogen combustion, the state-of-the-art thermal oil heater with external heating oil cycle has an efficiency of 89 % [31]. Thus, in this arrangement the minimum HCF is 37.5 %.

An Aspen Simulation shows that, due to full heat recuperation and stoichiometric air-fuel-ratio, the CHC heating concept avoids a very large part of the heat losses of the external heating oil cycle (see Fig. S1). Consequently, less hydrogen is required for combustion and more of the released hydrogen is available for the desired application. This increases the overall storage efficiency of the entire LOHC cycle.

In our study, the experimentally determined HCF values range

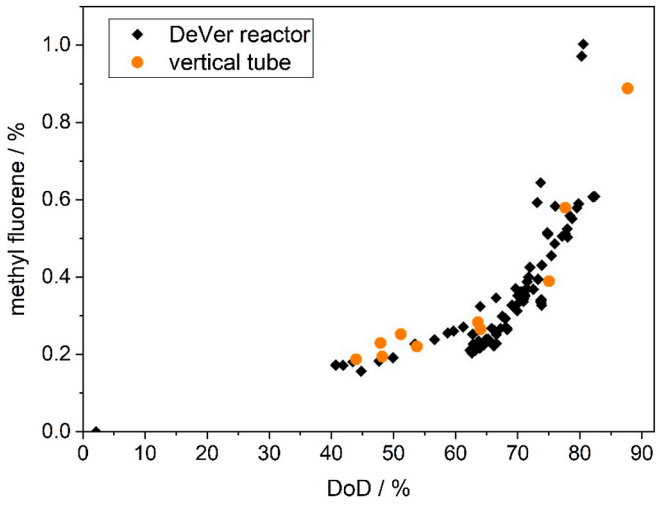

Fig. 5. Analysis of the liquid product Hx-BT from the DeVer reactor in comparison to the vertical tube. Depicting the methyl fluorene (MF) concentration as a function of the DoD for the two reactors DeVer and vertical tube shows that there is no increased MF formation in the DeVer reactor compared to the vertical tube [16].

Table 1
Comparison of the innovative CHC-based heating concept for LOHC dehydrogenation with conventional heating concepts based on thermal oil heating and electric heating.

heating concept	space requirement	energy consumption (HCF) [c]	explosion protection	zero NO_x emission
CHC	6 % of plant volume [28]	33 %	I. + II. explosion protection	yes
thermal oil heating [a]	30 % of plant volume [27]	37 % [d]	III. explosion protection	no
electric heating	1–2 % of plant volume [b]	55 % [e]	no risk of explosion	yes

[a] Thermal oil heating coupled with conventional hydrogen combustion.
[b] Assumption based on space consumption of electrical cabinet.
[c] The specific energy consumption required for heating the dehydrogenation in the form of HCF.
[d] Due to 10 % energy losses in state-of-the-art hydrogen fired thermal oil heaters.
[e] Due to 40 % energy losses in state-of-the-art fuel cells.

between 37 % and 55 %, with the reference configuration achieving an HCF = 42 %. The experimental data set is shown in the SI. For the reference configuration, the heat losses account for additional 9 %pt of the HCF. This is remarkable considering the relatively large heat losses in our small plant. For reference, the lab-scale dehydrogenation unit used by Wang et al. [20] consumed almost two thirds (65.1 %) of the released hydrogen for heating the dehydrogenation unit. However, these authors did not realize heat recuperation from the burner's hot exhaust gases. The goal of the autothermal reactor concept demonstrated in this work is ultimately to approach the ideal hydrogen combustion fraction of HCF = 33 % in a further scale-up of our autothermal H12-BT dehydrogenation concept.

3.1.3. LOHC stability and hydrogen quality

The LOHC samples taken after condensation of the product flow were analyzed for methyl fluorene content to evaluate by-product formation and LOHC reusability. Methyl fluorene is a deep dehydrogenation product that forms during oxidative cyclization from the hydrogen-lean LOHC compound H0-BT. For comparison, samples from a thermal oil-heated vertical tubular reactor (same catalyst, comparable conditions)

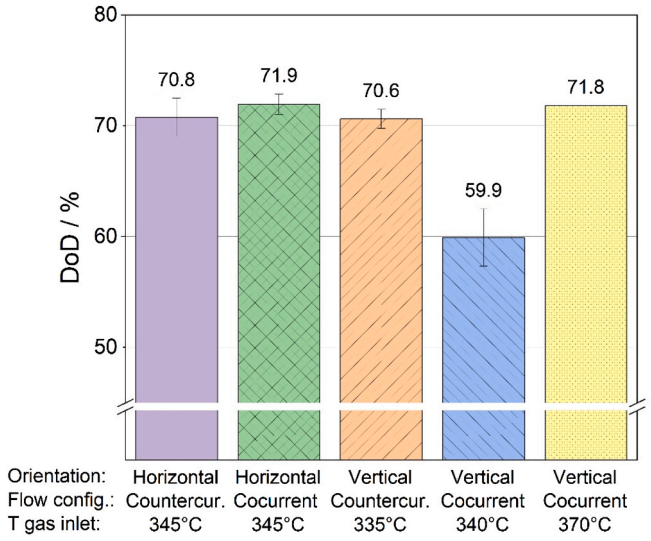

Fig. 6. Comparison of the tested reactor orientations and flow configurations regarding the achieved DoD in the reference configuration with similar gas inlet temperatures. With an adjustment of the gas inlet temperature (column 5), all setups reach a comparably high DoD, demonstrating the robust and flexible reactor design. The gas preheating tube temperature was kept constant at 350 °C. Because of changes in the setup for the different configurations, tube lengths changed, and the resulting gas inlet temperature was not the same.

[16] were analyzed with the same method in the same gas chromatograph. As shown in Fig. 5, the MF concentration as function of the product DoD shows a very similar course for both heating concepts.

This result is very encouraging as one could have assumed that the less uniform temperature distribution in the CHC compartment would lead to a higher amount of side products which was, however, not observed.

The released hydrogen was also analyzed for its quality subsequently to the LOHC vapor condensation unit. As expected, certain amounts of volatile organic compounds (VOCs), methane and CO were detected in the product gas. The VOC concentration in the released hydrogen in the CHC-heated reference configuration was 72 ppm, while the maximum total concentration of all impurities was always below 150 ppm for all our process configurations. This compares to literature values for an oil-heated inverted H12-dehydrogenation reactor for which under comparable process conditions VOC contents of over 300 ppm were measured prior to the active carbon adsorber [32]. While the exact cause for this difference in volatiles formations remains to be further investigated, we can safely state that the autothermal dehydrogenation using the CHC compartment as heating source does not increase the level of volatile impurities in the product hydrogen.

In summary, we found that direct heating by catalytic hydrogen combustion is at least equivalent to hot oil-heated reactor concepts in terms of gas and liquid product quality.

3.1.4. Safety

Another important benefit of an autothermal dehydrogenation reactor using CHC heating is enhanced intrinsic safety. CHC enables a controlled flameless oxidation reaction outside the explosive concentration range of the hydrogen-air mixture, mitigating the risk of unwanted ignitions or flame flashbacks [21,25,33]. Exhaust gas recirculation allows the CHC to operate outside the explosion regime while still maintaining stoichiometric combustion that leads to high combustion efficiency. Furthermore, the autoignition temperature of the combustion gas mixture is never exceeded in the CHC process. During the experiments of this study, the CHC process was operated at concentrations below 2.5 mol.-% O_2 and below 3.5 mol.-% H_2. The remainder was H_2O and N_2 from the gas recirculation. Using this feed

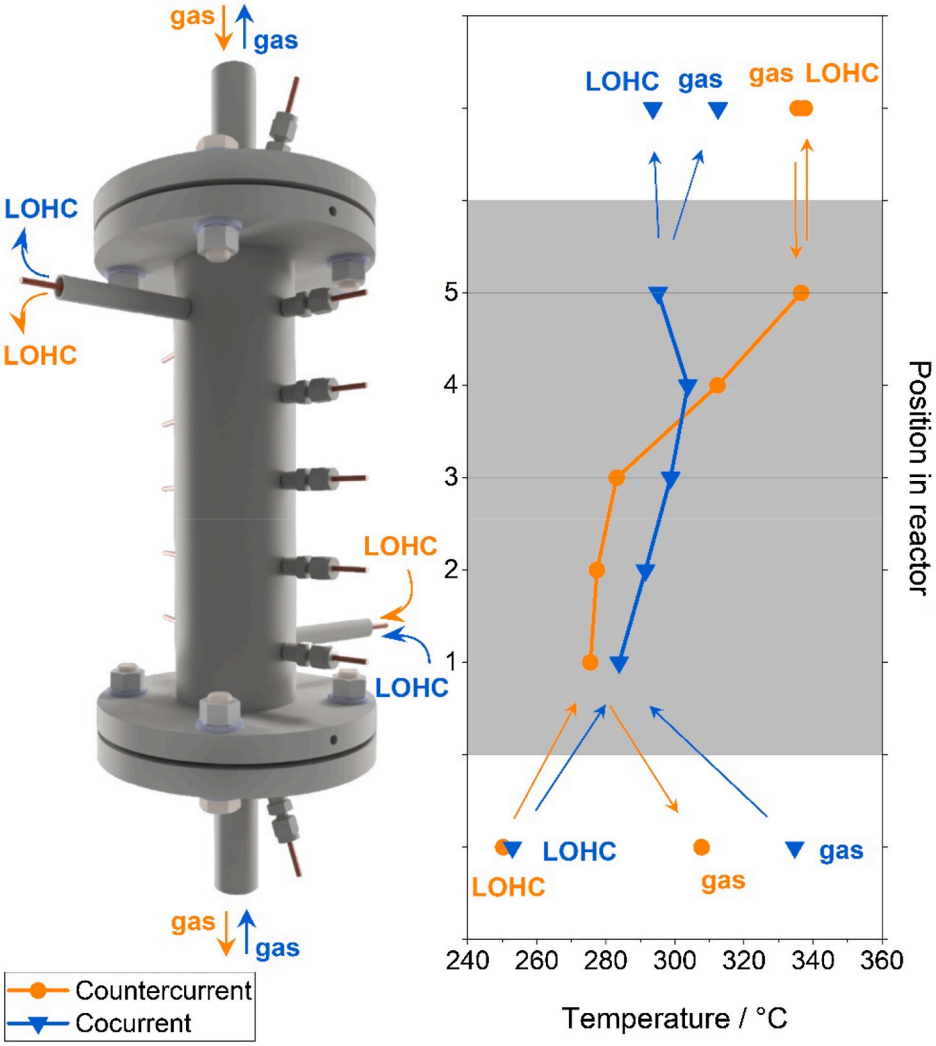

Fig. 7. Temperature profiles along the x-axis of the vertical dehydrogenation in operation. Co-current and counter-current operation mode is compared at reference configuration. The counter-current configuration (orange) shows better heat transfer characteristics and higher maximum temperatures compared to the co-current configuration. The given temperatures are mean temperatures from the three measurement points T_{ct}, T_{ot}, T_b. (For interpretation of the references to colour in this figure legend, the reader is referred to the Web version of this article.)

gas composition, the CHC compartment was operated in a stable manner over 110 h with CHC reactor temperatures below 400 °C. It can therefore be concluded that the combination of CHC with the exhaust gas recirculation provides an inherently safe heating concept for autothermal hydrogen release. The presented exhaust gas recycle reactor concept meets the demands of both primary and secondary explosion protection following the German regulation for hazardous and explosive substances (Technischen Regeln für Gefahrstoffe für den Explosionsschutz-TRGS 700er Reihe).

3.1.5. Emissions

While NO_x emissions are a serious issue for conventional free-flame hydrogen combustion processes where flame temperatures can reach values higher than 1500 °C, CHC provides a very clean combustion process at temperatures below 500 °C with zero NO_x formation [33].

Also, the concentration of VOC impurities in the exhaust gas of the combustion process is very low despite the fact that the hydrogen origins from the LOHC dehydrogenation process. Although the VOC concentration in the hydrogen product gas was 72 ppm in the reference configuration, we could not detect any VOC concentration in the exhaust gas after the CHC compartment. We assume that most of the VOCs in the hydrogen are converted to CO_2 during the CHC process. In experiments with purposedly increased VOC concentration, we could confirm that always more than 80 % of the VOCs were converted to CO_2 (Figure S5 a). Additionally, we did not see a detrimental effect on hydrogen conversion during a longtime experiment over ca. 200 h (Figure S5 b). With the measured VOC concentrations in the product hydrogen gas we can confirm that the emission limits for VOCs as regulated by TA-Luft ($c_{Benzene,H2} < 0.5$ mg m^{-3}, $c_{Toluene,H2} < 1$ mg m^{-3}) are met for the CHC exhaust gas [34].

Note that the minimal amounts of CO_2 that origin from the combustion of VOCs from the LOHC dehydrogenation compartment are far below the limits that the EU has set for renewable hydrogen if the Hx-BT has been initially charged with clean hydrogen (no CO_2 emission related to the hydrogen production). According to EU directives, hydrogen is labelled renewable if it saves at least 70 % greenhouse gas emissions compared to hydrogen from fossil sources [35–37]. The hydrogen product flow from the H12-BT dehydrogenation compartment is separated into a cleaned flow for hydrogen utilization (67 %) and into a hydrogen flow for combustion (33 %). Based on the VOCs level in the hydrogen gas product, the CO_2 emissions per kilogram useable hydrogen released would be at ca. 0.07 $kg_{CO2}\ kg_{H2}^{-1}$ which is far below the emission limit for renewable hydrogen in the EU that ranges between 2.25 and 3.9 $kg_{CO2}\ kg_{H2}^{-1}$ (depending on the reference value of CO_2 emissions for gray

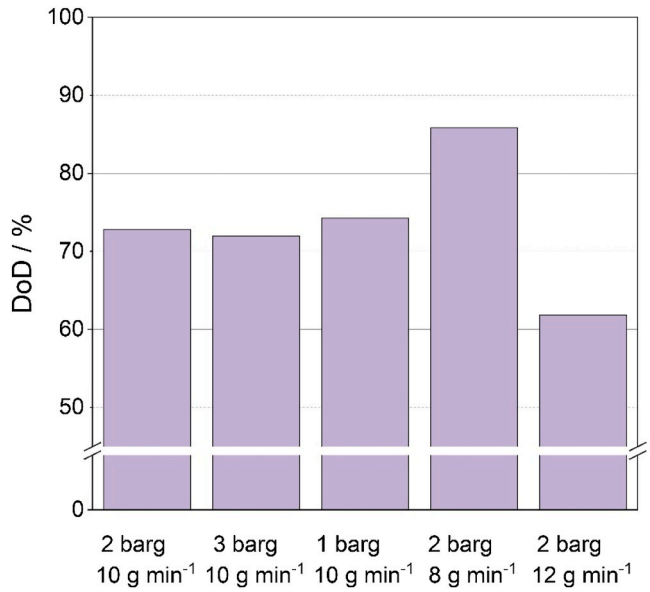

Fig. 8. Influence of reactor pressure and H12-BT flow on the DoD at reference configuration. A higher pressure leads to a slightly decreased DoD. A decreased H12-BT flow results in a higher residence time and thus a higher DoD.

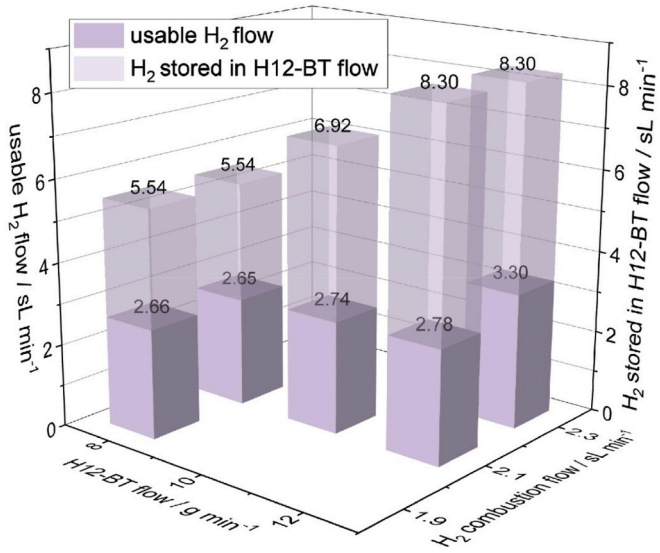

Fig. 9. Influence of H12-BT and H_2 combustion flow rates on the released, useable H_2 flow in relation to the H_2 flow that is stored in the LOHC, demonstrating the high flexibility of the process design. By raising the H12-BT and H_2 combustion flow the useable H_2 flow can be increased in times of high H_2 demands, while the best ratio of useable H_2 per stored H_2 flow, i.e., the best storage efficiency, is reached at low H12-BT and H_2 combustion flows.

hydrogen) [[37,38]]. Consequently, hydrogen from the here-described autothermal dehydrogenation process would be labelled renewable hydrogen in accordance with EU regulations.

To summarize, Table 1 presents the described characteristics of a CHC-heated H12-BT dehydrogenation process in comparison to thermal oil-heated or electrically heated concepts.

3.2. Performance for different process configurations

We like to describe now the performance of the proposed CHC-heated dehydrogenation reactor under varying process configurations and conditions. For this purpose, we refer to the KPIs defined above.

3.2.1. Reactor orientation and flow direction

The influence of the reactor orientation and flow configuration on the DoD was investigated for the reference process conditions. The slight variation in gas inlet temperatures for the first four columns is due to small differences in the pipe connections and insulation among the different setups. As depicted in Fig. 6, horizontal and vertical orientation of the CHC-heated H12-BT dehydrogenation reaction as well as co- and countercurrent flows showed almost no difference regarding the achieved DoD. Only the vertical orientation with cocurrent operation resulted in a significantly lower DoD than the other setups.

By increasing the gas inlet temperatures, the temperature level in the dehydrogenation unit increases. With 370 °C inlet temperature the vertical co-current setup reaches very similar DoDs to the other setups with around 340 °C.

3.2.2. Temperature profile

Fig. 7 shows a comparison of the temperature distribution along the reactor axis for the two flow configurations, co-current and counter-current, in the vertical reactor orientation. In the counter-current configuration (orange plot) the gas and LOHC temperatures on the low temperature side are on average significantly lower than on the high temperature side, where gas and LOHC temperatures are almost identical ($T_{counter,LOHC,out} = 337.6\,°C$; $T_{counter,gas,in} = 335.5\,°C$). The co-current configuration (blue plot) results in a more even temperature along the reactor x-axis. The gas and LOHC temperatures on the high temperature side are wider spread than in the counter-current configuration. This shows that a smaller part of the thermal energy in the gas is transferred to the LOHC mixture in the co-current mode compared to the counter-current mode ($T_{co,LOHC,out} = 293.6\,°C$; $T_{co,gas,out} = 312.5\,°C$) [39].

The less efficient heat transfer also results in a higher gas outlet temperature for the cocurrent configuration ($T_{co,gas,out} = 312.5\,°C$) compared to the countercurrent configuration ($T_{co,gas,out} = 307.7\,°C$). As a consequence, the resulting maximum temperature in the reactor is higher in the counter-current configuration, which leads to a higher DoD and a lower fraction of the released hydrogen has to be fed to the CHC compartment ($HCF_{vertical,co} = 49.3\,\%$; $HCF_{vertical,counter} = 42.3\,\%$). Thus, the amount of useable, released hydrogen is higher for the countercurrent configuration than for the cocurrent configuration.

In contrast, no significant difference in the temperature profiles for counter-current vs co-current operation mode was detected for the horizontal reactor orientation (see Fig. S3). A possible reason for this effect can be found in the reactor design. In the horizontal setup it is assumed that on the shell side the pre-heated H12-BT enters the reactor at the bottom where it builds a predominantly liquid reservoir. When heated up by the CHC process, hydrogen is being released and the LOHC compounds pass partly into the gas phase, rising to the top of the reactor, where the outlet is located. Thus, a LOHC flow from the bottom to the top is formed, running crosswise to the hydrogen combustion flow in the tubes that are aligned horizontally. This crossflow presumably results in the observed temperature profile that shows better heat transfer characteristics as well as higher maximum temperatures and consequently higher DoDs, compared to the vertical cocurrent setup, which by comparison is a true parallel flow. The temperature distribution with all temperature points (T_{ct}, T_{ot}, T_b) is exemplary shown for one experiment at reference configuration in Fig. S4.

3.2.3. Reactor pressure and H12-BT flow

The influence of the process parameters pressure and H12-BT flow on the achieved DoD is shown in Fig. 8.

The effect of the process pressure on the DoD is surprisingly small due to two counteracting effects. On the one hand, decreasing reaction pressure reduces the hydrogen partial pressure in the rector, which is beneficial for the driving force of the H12-BT dehydrogenation. On the other hand, lower hydrogen partial pressure enhances evaporation of

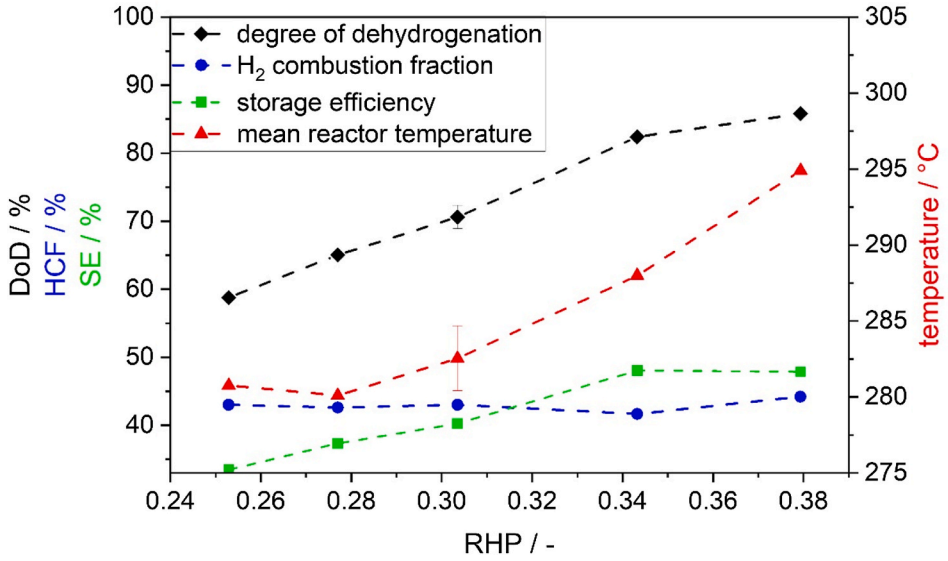

Fig. 10. Behavior of KPIs with varying relative heating power ($\dot{H}_C/\dot{H}_S$), showing a correlation between reactor temperature and DoD as well as storage efficiency. It indicates that, during an alteration of process parameters, the resulting reactor temperature is the key factor that consequently determines the DoD and with that, finally, the overall storage efficiency of the system. Reaction conditions: dehydrogenation side: $m_{H12\text{-}BT}$ = 8–12 g min^{-1}, p_{dehy} = 2 barg, $T_{H12\text{-}BT\ tube\ preheating}$ = 350 °C; combustion side: $T_{gas\ tube\ preheating}$ = 350 °C, 70 sL min^{-1}, 2.7–3.3 % H_2, 2 % O_2, 64 % N_2, 31 % H_2O. Error bars show the standard deviation from 9 reference operation points ($m_{H12\text{-}BT}$ = 10 g min^{-1}, 3 % H_2).

H12-BT, which reduces the average feedstock residence time in the reactor [19]. A larger effect on DoD shows, in contrast, a variation of the H12-BT flow rate through the reactor. Variation of the H12-BT flow from the reference configuration (2 barg, 10 g min^{-1}) to lower H12-BT flow (2 barg, 8 g min^{-1}) or higher H12-BT flow (2 barg, 12 g min^{-1}) changes the DoD by + 12.4 %pt and – 14.6 %pt, respectively. This is explained by the higher (lower) average residence time for lower (higher) h12-BT flow rates resulting in higher (lower) DoDs.

3.3. Process control and storage efficiency

Fig. 9 summarizes the performance of our autothermal reactor under varying H12-BT and hydrogen combustion flow rates in the respective reactor compartments.

It shows that the ratio of released useable hydrogen flow to the stored hydrogen flow is strongly influenced by the H12-BT and hydrogen combustion flow rates. Higher H12-BT flow and hydrogen combustion flow rates lead to slightly larger useable hydrogen flows while the DoD goes down. The highest storage efficiency, i.e., the highest ratio of useable hydrogen flow to hydrogen stored in the LOHC feedstock flow is found in the applied experimental configuration at 8 g min^{-1} H12-BT and 1.9 sL min^{-1} hydrogen combustion flow. Although the absolute flow of useable released hydrogen is smaller in this configuration, a relatively large fraction of 48 % of the hydrogen stored in the LOHC is available for usage. This value considers both the hydrogen needed for heat provision and the hydrogen that remain bound to the LOHC carrier after dehydrogenation due to the incomplete dehydrogenation (DoD <100 %). For the operation points with higher absolut hydrogen output, lower storage efficiencies are found with 39.8 % being the lowest storage efficiency at 12 g min^{-1} H12-BT flow and 2.3 sL min^{-1} in our configuration. These results prove a certain load flexibility of our autothermal dehydrogenation reactor by adjustent of the H12-BT and the hydrogen combustion flow rates.

In Fig. 10 the behavior of the process is plotted over the relative heating power (RHP), i.e., the ratio of hydrogen combustion flow per stored hydrogen in the H12-BT flow.

The data points presented on the x-axis refer to the five configurations displayed in Fig. 10. There is an obvious correlation between mean reactor temperature and the reached DoD for a variation of the relative heating power. We assumed that equivalent to the reactor orientation and flow direction variation, the main reason for a change in DoD during an alteration of process parameters is the resulting temperature change in the reactor. With increased relative heating power, the resulting mean reactor temperature rises, and a higher DoD is reached in the dehydrogenation reaction. At the same time, the relative hydrogen combustion fraction stays almost constant at 42–44 %, leading to an increase in storage efficiency for rising relative heating power. Techno economically attractive DoDs >80 % are reached at reactor temperatures higher than 295 °C with storage efficiencies of around 45 % realized in our experimental autothermal reactor configuration [12].

4. Conclusion

In this study, we propose a novel reactor concept for autothermal dehydrogenation of liquid organic hydrogen carriers (LOHCs) that combines catalytic hydrogen combustion (CHC) and H12-BT dehydrogenation in an inverted reactor design. Compared to conventional free-flame hydrogen combustion, CHC allows for operation at moderate temperatures, eliminating the need for a thermal oil cycle and reducing the required space by up to 80 %. In our experiments, the applied lab-sized autothermal reactor achieved a peak storage efficiency of 48 % and a minimum hydrogen combustion fraction of 37 %. Both parameters should further increase if the system is scaled up as heat losses are becoming less relevant in larger devices.

Our results indicate that the proposed reactor configuration can produce hydrogen in high quality and maintain the recyclability of the applied LOHC carrier system. Compared to more traditional dehydrogenation reactor configurations, no elevated side product formation, i.e. methyl fluorene formation, was observed. The emission of volatile organic compounds (VOCs) and CO_2 was found to be similar or even lower in our new autothermal setup. The proposed autothermal reactor meets the demands of both primary and secondary explosion protection enabling industrial and mobile application.

In experimental series under variation of process parameters and flow configurations, we could demonstrate the stability and adaptability of the autothermal reactor concept. The temperature level in the reactor was found to have the main influence on the degree of dehydrogenation and the storage efficiency.

Our results demonstrate that the proposed autothermal hydrogen release concept offers several advantages over state-of-the-art heating concepts, including electrical heating and conventional hydrogen combustion with circulating thermal oil. The combination of CHC and dehydrogenation in an inverted reactor design enables hydrogen provision from H12-BT with high volumetric power density, minimal heat losses (even in laboratory equipment) and safe process operation.

CRediT authorship contribution statement

C. Gescher: Writing – original draft, Visualization, Investigation, Formal analysis, Data curation. **S. Hahn:** Writing – review & editing, Validation, Methodology, Investigation, Formal analysis, Data curation, Conceptualization. **C. Hornung:** Writing – review & editing, Investigation, Formal analysis, Data curation. **M. Weiss:** Writing – review & editing, Investigation, Data curation. **T. Rüde:** Writing – review & editing, Supervision, Project administration, Methodology. **M. Geißelbrecht:** Writing – review & editing, Validation, Supervision, Resources, Project administration. **P. Wasserscheid:** Writing – review & editing, Supervision, Resources, Project administration, Methodology, Funding acquisition, Conceptualization.

Declaration of competing interest

Peter Wasserscheid is founder and minority share holder of the company Hydrogenious LOHC Technologies (www.hydrogenious.net) that offers commercially hydrogen storage systems based on the LOHC technology.

There is no conflict of interest to declare with regard to the specific scientific results reported in this paper.

Acknowledgements

The authors acknowledge financial support by the Bavarian Ministry of Economic Affairs, Regional Development and Energy through the project “Emissionsfreier und stark emissionsreduzierter Bahnverkehr auf nicht-elektrifizierten Strecken”. In addition, the authors gratefully acknowledge support by the LNG2Hydrogen project as part of the TransHyDE hydrogen flagship project (funding code: 03HY210 I). The authors further acknowledge financial support by the German Federal Ministry of Research, Technology and Space (BMFTR) through the HyFRed project (funding code: 03SF0746A).

Appendix A. Supplementary data

Supplementary data to this article can be found online at https://doi.org/10.1016/j.ijhydene.2025.151694.

References

[1] Lee H. Climate change 2023 synthesis report. 35–115, https://doi.org/10.59327/IPCC/AR6-9789291691647; 2023.
[2] Schweizer bundesamt für energie 2021 - Energiespeichertechnologien.pdf n.d.
[3] Stadler I, Sterner M. Urban energy storage and sector coupling. Urban Energy Transit Renew Strateg Cities Reg 2018:225–44. https://doi.org/10.1016/B978-0-08-102074-6.00026-7.
[4] Schüth F. Chemical compounds for energy storage. Chem Ing Tech 2011;1984–93. https://doi.org/10.1002/cite.201100147.
[5] Dutta S. A review on production, storage of hydrogen and its utilization as an energy resource. J Ind Eng Chem 2014;20:1148–56. https://doi.org/10.1016/j.jiec.2013.07.037.
[6] Capurso T, Stefanizzi M, Torresi M, Camporeale SM. Perspective of the role of hydrogen in the 21st century energy transition. Energy Convers Manag 2022;251:114898. https://doi.org/10.1016/j.enconman.2021.114898.
[7] Usman MR. Hydrogen storage methods: review and current status. Renew Sustain Energy Rev 2022;167:112743. https://doi.org/10.1016/j.rser.2022.112743.
[8] Preuster P, Papp C, Wasserscheid P. Liquid organic hydrogen carriers (LOHCs): toward a hydrogen-free hydrogen economy. Acc Chem Res 2017;50:74–85. https://doi.org/10.1021/acs.accounts.6b00474.
[9] Bollmann J, Schmidt N, Beck D, Preuster P, Zigan L, Wasserscheid P, et al. A path to a dynamic hydrogen storage system using a liquid organic hydrogen carrier (LOHC): burner-Based direct heating of the dehydrogenation unit. Int J Hydrogen Energy 2023;48:1011–23. https://doi.org/10.1016/j.ijhydene.2022.09.234.
[10] Staiß F, Adolf J, Ausfelder F, Erdmann C, Fischedick M, Hebling C, et al. Optionen Für Den Import Grünen Wasserstoffs Nach Deutschland Bis Zum Jahr 2030 : Transportwege - Länderbewertungen - Realisierungserfordernisse. 2022.
[11] Weichenhain U. Hydrogen transportation. The key to unlocking the clean hydrogen economy. Rol Berger; 2021. p. 1–28.
[12] Distel MM, Margutti JM, Obermeier J, Nuß A, Baumeister I, Hritsyshyna M, Weiß A, Neubert M. Large-scale H2 storage and transport with liquid organic hydrogen carrier technology: insights into current project developments and the future outlook. Energy Technol 2024:2301042. https://doi.org/10.1002/ente.202301042.
[13] IRENA (International Renewable Energy Agency). Global hydrogen trade to meet the 1.5°C climate goal. Technology Review Of Hydrogen Carriers. 2022.
[14] Rüde T, Dürr S, Preuster P, Wolf M, Wasserscheid P. Benzyltoluene/Perhydro benzyltoluene - pushing the performance limits of pure hydrocarbon liquid organic hydrogen carrier (LOHC) systems. Sustain Energy Fuels 2022;6:1541–53. https://doi.org/10.1039/d1se01767e.
[15] Peters R, Deja R, Fang Q, Nguyen VN, Preuster P, Blum L, et al. A solid oxide fuel cell operating on liquid organic hydrogen carrier-based hydrogen – a kinetic model of the hydrogen release unit and system performance. Int J Hydrogen Energy 2019;44:13794–806. https://doi.org/10.1016/j.ijhydene.2019.03.220.
[16] Willer M, Preuster P, Geißelbrecht M, Wasserscheid P. Continuous dehydrogenation of perhydro benzyltoluene and perhydro dibenzyltoluene in a packed bed vertical tubular reactor – the role of LOHC evaporation. Int J Hydrogen Energy 2024;57:1513–23. https://doi.org/10.1016/j.ijhydene.2024.01.031.
[17] Niermann M, Drünert S, Kaltschmitt M, Bonhoff K. Liquid organic hydrogen carriers (LOHCs)-techno-economic analysis of LOHCs in a defined process chain. Energy Environ Sci 2019;12:290–307. https://doi.org/10.1039/c8ee02700e.
[18] Siegert F, Gundermann M, Maurer L, Hahn S, Hofmann J, Distel M, et al. Autothermal hydrogen release from liquid organic hydrogen carrier systems. Int J Hydrogen Energy 2024;91:834–42. https://doi.org/10.1016/j.ijhydene.2024.10.044.
[19] Kadar J, Gackstatter F, Ortner F, Wagner L, Willer M, Preuster P, et al. Boosting power density of hydrogen release from LOHC systems by an inverted fixed-bed reactor design. Int J Hydrogen Energy 2024;59:1376–87. https://doi.org/10.1016/j.ijhydene.2024.02.096.
[20] Wang S, Si H, Li P, Cao C. Towards maximum hydrogen output from methylcyclohexane dehydrogenation coupled with catalytic hydrogen combustion: an experimental and simulation study. Int J Hydrogen Energy 2025;98:807–19. https://doi.org/10.1016/j.ijhydene.2024.12.138.
[21] Kim J, Yu J, Lee S, Tahmasebi A, Jeon CH, Lucas J. Advances in catalytic hydrogen combustion research: catalysts, mechanism, kinetics, and reactor designs. Int J Hydrogen Energy 2021;46:40073–104. https://doi.org/10.1016/j.ijhydene.2021.09.236.
[22] Nguyen VN, Deja R, Peters R, Blum L, Stolten D. Study of the catalytic combustion of lean hydrogen-air mixtures in a monolith reactor. Int J Hydrogen Energy 2018;43:17520–30. https://doi.org/10.1016/j.ijhydene.2018.07.126.
[23] Kozhukhova AE, du Preez SP, Bessarabov DG. Catalytic hydrogen combustion for domestic and safety applications: a critical review of catalyst materials and technologies. Energies 2021;14. https://doi.org/10.3390/en14164897.
[24] Fumey B, Buetler T, Vogt UF. Ultra-low NOx emissions from catalytic hydrogen combustion. Appl Energy 2018;213:334–42. https://doi.org/10.1016/j.apenergy.2018.01.042.
[25] Saint-Just J, Etemad S. Catalytic combustion of hydrogen for heat production. Compend Hydrog Energy Hydrog Energy Convers 2015;3(3):263–87. https://doi.org/10.1016/B978-1-78242-363-8.00010-4.
[26] Hahn S. German Patent no. 10 2023 200 245, Expected Release Date: 14.07.2024. Ger Pat No 10 2023 200 245; Expect Release Date 14072024 2023.
[27] Regele C, Gackstatter F, Ortner F, Preuster P, Geißelbrecht M. Simulation and optimisation of a LOHC-Based hydrogen train system. Energy Convers Manag 2025;344:120234. https://doi.org/10.1016/j.enconman.2025.120234.
[28] Hahn S. Sichere, emissionsfreie und effiziente Wärmebereitstellung mit Hilfe einer flammenlosen. katalytischen Wasserstoffverbrennung, https://doi.org/10.25593/open-fau-1850; 2025.
[29] Hydrogenious LOHC Technologies GmbH. Our LOHC technology – disrupting hydrogen infrastructure. https://archive.ph/CvwsD; 2024.
[30] Hydrogenious LOHC Technologies GmbH. Technology of hydrogenious. https://archive.ph/hlzap; 2024.
[31] Manufacturer of thermal oil heaters. Engeneering Eines 600 Kw Wasserstoffbetriebenen Thermalölerhitzers. 2024.
[32] Zilm A, Ortner F, Gackstatter F, Köberlein S, Kadar J, Geißelbrecht M, Bösmann A, Wasserscheid P. Impurities in hydrogen released from perhydro benzyltoluene - assessment and adsorptive removal. Int J Hydrogen Energy 2025;101:469–81. https://doi.org/10.1016/j.ijhydene.2024.12.204.
[33] du Preez SP, Jones DR, Bessarabov DG, Falch A, Mota das Neves Quaresma C, Dunnill CW. Development of a Pt/stainless steel mesh catalyst and its application in catalytic hydrogen combustion. Int J Hydrogen Energy 2019;44:27094–106. https://doi.org/10.1016/j.ijhydene.2019.08.168.
[34] Neufassung der Ersten Allgemeinen Verwaltungsvorschrift zum Bundes-Immissionsschutzgesetz. Technische Anleitung zur Reinhaltung der Luft – TA Luft). GMBl 2021:1050.
[35] European Commission. Commission delegated regulation supplementing directive (EU) 2018/2001 of the European parliament and of the council. By establ a minim treshold GHG emiss savings recycl carbon fuels by specif a methodol assess GHG

savings from renew liq gaseous transp fuels No-Biological orig from. Recycl Carbon Fuels 2023:12–26.
[36] European Commission. Commission delegated regulation (eu) 2023/1185 of 10 February 2023 supplementing directive (EU) 2018/2001 of the european parliament and of the council by establishing a minimum threshold for greenhouse gas emissions savings of recycled carbon fuels and b 2023;vol.1185:20–33.
[37] European Commission. Directive (EU) 2023/2413 of the european parliament and of the council of 18 October 2023 amending directive (EU) 2018/2001, regulation (EU) 2018/1999 and directive 98/70/EC as regards the promotion of energy from renewable sources. Off J Eur Union 2023;2413:1–77.
[38] Incer-Valverde J, Korayem A, Tsatsaronis G, Morosuk T. "colors" of hydrogen: definitions and carbon intensity. Energy Convers Manag 2023;291. https://doi.org/10.1016/j.enconman.2023.117294.
[39] Verein Deutscher Ingenieure V-GV und C (GVC). VDI wärmeatlas. ninth ed. Heidelberg: Springer Berlin; 2013. https://doi.org/10.1007/978-3-662-10743-0.